

The ECMWF Model Climate: Recent Progress Through Improved Physical Parametrizations

**Thomas Jung¹, Gianpaolo Balsamo¹, Peter Bechtold¹, Anton Beljaars¹,
Martin Köhler¹, Martin Miller¹, Jean-Jacques Morcrette¹, Andrew Orr^{1,3},
Mark Rodwell¹ and Adrian M. Tompkins^{1,2}**

¹ *ECMWF, Shinfield Park, Reading RG2 9AX, United Kingdom*

² *ICTP, Strada Costiera 11, 34014 Trieste, Italy*

³ *BAS, High Cross, Madingley Road, Cambridge CB3 0ET, United Kingdom*

ABSTRACT

The progress achieved since 2005 in simulating today's climate with the ECMWF model through improved physical parametrizations is described. Results are based on climate integrations at an intermediate horizontal resolution (T_L159) using model cycles employed operationally at ECMWF since June 2005. It turns out that recent improvements to the physical parametrization package led to substantial reductions of long-standing systematic model error including tropical precipitation, convectively coupled tropical waves, the circulation in the Northern Hemisphere extratropics including synoptic-scale variability, Euro-Atlantic blocking and the North Atlantic Oscillation.

1 Introduction

A frequently asked question is how well state-of-the-art atmospheric models simulate today's climate and how systematic errors have changed in time through improvements in model formulation (e.g. [Jung, 2005](#); [Reichler and Kim, 2008](#)). An assessment of three generations of coupled models, which took part in three coupled model intercomparison projects (CMIP), by [Reichler and Kim \(2008\)](#) shows that atmospheric components of state-of-the-art models are certainly not perfect but certainly better than their predecessors; the authors explain this improvement by the introduction of realistic model formulations and increased horizontal and vertical resolution.

A comprehensive study of systematic errors in the ECMWF model and their evolution from the 1980s has been presented by [Jung and Tompkins \(2003\)](#), [Jung \(2005\)](#) and [Jung et al. \(2005b\)](#). These studies revealed substantial improvements, particularly during the 1980s and 1990s, of systematic errors in the medium-range. The then operational model cycle (cycle 26R1, operational in 2003), however, produced still substantial errors in climate integrations such as pronounced underestimation of synoptic activity in high-latitudes, underestimation of the frequency of occurrence Euro-Atlantic blocking, a strong anti-cyclonic circulation bias in the North Pacific and short-comings in the tropical hydrological cycle.

Since 2003 considerable effort has been devoted at ECMWF to improving the physical parametrization package in order to reduce the above-mentioned model problems. The aim of this study is to give an overview of the model changes introduced since June 2005 and to assess their impact on the climate of the ECMWF model. As it turns out, recent improvements have been highly beneficial in terms of alleviating many of the long-standing problems found in the ECMWF model (and more generally in other models).

The paper is structured as follows: The experimental setup and a description of the model changes introduced since June 2005 will be given in section 2. This is followed by the Results section in which systematic errors and their changes are discussed for precipitation, the extratropical circulation including extratropical cyclones and blocking, the North Atlantic Oscillation and tropical convectively coupled waves. Finally, the results are

Table 1: Main characteristics of the datasets used in this study. Values of the resolution given in parentheses are approximate values in degrees latitude/longitude.

Cycle	Introduced	Modifications
29R2	2005/06/28	Modification to convection scheme
30R1	2006/02/01	Increased vertical resolution (L60 to L91)
31R1	2006/09/12	Revised cloud scheme (ice supersaturation + numerics); implicit computation of convective transports; introduction of turbulent orographic form drag (TOFD) scheme; revised parameterization of sub-grid scale orographic drag
32R1	not operational	New short-wave radiation scheme; introduction of McICA cloud radiation interaction MODIS land surface albedo; retuned ice particle size; retuning of GWD (increase by a factor of two)
32R2	2007/06/05	Minor changes to the forecast model
32R3	2007/11/06	New formulation of convective entrainment and relaxation time scale; reduced vertical diffusion in the free atmosphere; modification to GWD scheme at the top of the model; new soil hydrology scheme
33R1	2008/06/03	Slightly increased vertical diffusion; increased orographic form drag; retuned entrainment in the convection scheme bugfix scaling of freezing term in convection scheme changes to surface model

discussed in section 4.

2 Method

2.1 Experimental design

The realism of the ECMWF model climate was assessed using 13 month long integrations with model cycles used operationally at ECMWF since June 2005. The model cycles along with their key-changes are summarized in Table 1; a more detailed description of the changes will be given in the following section.

All integrations were carried out using observed SST and sea ice fields as lower boundary conditions. Forecasts were started on 1 November of each of the years 1962–2005. The standard meteorological seasons (DJF, MAM, JJA and SON) were diagnosed. In this study, however, the focus will be on boreal winter. All integrations were carried out employing a horizontal resolution of T_L159 (about 1.1°). Integrations with cycle 29R2 were carried out using 60 levels in the vertical. For model cycle 30R1 and more recent cycles the 91 level version, which was introduced into operations in February 2006 (Untch et al., 2006), was used.

Additional sensitivity experiments were carried out for winters of the period 1990–2005 in order to understand which of the changes that were introduced in cycle 32R3 were responsible for the substantial improvements found for this cycle in terms of the simulated model climate.

2.2 Description of recent parametrization changes

In the following a more detailed description of key-model changes listed in Table 1 will be given.

2.2.1 Orography

The Turbulent Orographic Form Drag (TOFD) parametrization (Beljaars et al., 2004b) was introduced in the ECMWF model in September 2006 (model cycle 31R1) to represent drag on the flow due to sub-grid scale orography (SSO) with horizontal scales below 5000 m. TOFD is an alternative to the previously used “effective roughness length” concept. The scheme is controlled by the standard deviation of subgrid orography in the scale range of 2 to 20 km, derived from a 1 km orographic data set. The desired spectral range of sub-grid scale orography with scales smaller than 5000 m is obtained by assuming a universal power spectrum. In cycle 33R1 the constant of proportionality, α , in the TOFD parametrization, has been increased from 12 to 27 (see Eqn. (15) in Beljaars et al. (2004b)), which is equivalent to an increase of the standard deviation of the SSO scheme by a factor 1.5.

Cycle 31R1 included a ‘cutoff’ or ‘effective’ mountain height in the computation of gravity wave drag from the SSO scheme. The more physically realistic cutoff mountain height resulted in a decrease in gravity wave drag (GWD), reducing the excessive deceleration of flow over the Himalayas and Rockies (Orr, 2007). However, climate runs showed an increase in the positive zonal wind bias over winter northern hemisphere mid-latitudes, suggesting that the reduction in GWD had been excessive. This problem was solved in cycle 32R1 by doubling the ‘cutoff’ mountain height and thereby increasing the amplitude of the gravity waves generated by the SSO scheme by a factor of two.

TOFD, SSO gravity wave drag and low-level blocking momentum tendencies can be significant over orography, resulting in quite large increments when the model time step is long. Moreover, to some extent the processes are coupled, leading to a time step sensitivity if each of the relative parameterization schemes evaluates its tendencies independently (Beljaars et al., 2004a). However, some degree of dependency (and a corresponding reduction in time step sensitivity) was introduced in cycle 31R1 by solving the relevant momentum tendency coefficients in a joint implicit calculation (Orr, 2007).

2.2.2 Radiation

A new package of radiation transfer parametrizations was introduced in the ECMWF IFS with cycle 32R1. It includes the short-wave part of the Rapid Radiation Transfer Model (RRTM: Iacono et al., 2008) (complementing the long-wave part of RRTM (Mlawer et al., 1997) introduced into the IFS in June 2000), the Monte-Carlo Independent Column Approximation (McICA: Barker et al., 2002; Pincus et al., 2003), revised ice cloud radiative properties, and a more extensive use of a reduced radiation grid. Impact of this new radiation package in one-year simulations at low resolution, in high-resolution 10-day and EPS 15-day forecasts is discussed in Morcrette et al. (2008a,b).

The recent introduction of the McRad package (Morcrette et al., 2008b) in the IFS has increased the cost of the radiation computations and required revisiting the use of the interface between radiation and the rest of the model, for the various meteorological applications run at ECMWF. A flexible interface introduced in 2003 allows for delocalized radiative computations with a potential increase in the computer efficiency of the model through a spatial representation of the radiation transfer differing from that of the other physical processes (Morcrette et al., 2008b).

2.3 Vertical diffusion

Turbulent diffusion in the stable boundary layer and in the free troposphere used in many models, including the ECMWF model, is larger than expected from local Monin-Obukhov (MO) similarity theory (e.g. [Louis et al., 1982](#), LTG). In order to increase the realism of the ECMWF model the diffusion coefficients in the ECMWF model were reduced to values consistent with MO theory in cycle 32R3 (see [Bechtold et al., 2008](#), for details). This change led to stronger shears and inversions, more stratocumulus (10–30% locally), colder ($-0.3K$) and moister ($0.1g\,kg^{-1}$) land surface, stronger ageostrophic winds and larger baroclinic growth rates.

In cycle 33R1 the vertical diffusion scheme was further modified by increasing turbulent transports above the surface layer. The motivation for this increase was twofold. First, power spectra of vertical shear in ECMWF model simulations at resolutions from T_L95 to T_L2047 indicate too little shear at small scales. This shear deficiency, which amounts to about 20%, peaks at around 850hPa. Parameterising this shear component in the diffusion coefficient explains about half of the LTG diffusion increase over MO theory. Second, we noted that the TOFD parameterization is working sub-optimal when coupled with MO diffusion coefficients. An adjustment of the TOFD coefficients, which represents the effect of small scale orography, significantly outperforms the empirically increased diffusion coefficients by LTG.

2.3.1 Large-scale cloud scheme

In cycle 31R1 a number of changes were implemented to the cloud scheme physics and numerics. The numerical changes were made necessary by the earlier increase in vertical resolution from 60 to 91 levels in the cycle 30R1 release. This revealed a significant vertical resolution sensitivity of the model climate at high resolutions, due to a combination of the ice microphysical assumptions and the previous cloud scheme numerical solution methodology (see [Tompkins, 2008](#), for details).

The numerical solver for the prognostic cloud water equation was therefore changed to use an forward-in-time upstream implicit solution. In conjunction with this, the previous cloud ice microphysical assumptions that ice settling into sub-cloud clear air was converted into snow were updated. Instead, from cycle 31R1, ice settling into sub-saturated cloud free air would undergo sublimation, while the conversion of ice to snow was handled by an explicit autoconversion parametrization. This used the parametric form of [Sundqvist et al. \(1989\)](#) that already represented warm rain processes, with [Lin et al. \(1983\)](#) rate constants that were adjusted for use in a large-scale rather than cloud resolving model, and also to minimize the change in climate and maximize forecast medium range skill.

At the same time, the opportunity was taken to reject the model assumption that no supersaturation can exist, in favour of a new cloud parametrization that permits supersaturation in clear sky part of gridboxes at cold temperatures below 235K at which homogeneous nucleation occurs. The supersaturation in clear sky is the most important to represent since, once ice nucleation has occurred, and especially by homogeneous nucleation processes which produce high ice number concentrations with respect to heterogeneous nucleation ([Demott et al., 2003](#)), the rapid growth of ice crystals by deposition reduces the in-cloud supersaturation back towards negligible levels within a typical GCM timestep in all dynamical circumstances bar the strongest of updraughts ([Lohmann and Kärcher, 2002](#); [Gierens, 2003](#)). Moreover, attempting to include a representation of the in-cloud supersaturation requires a separate (prognostic) memory of the evolution of water vapour within and outside the cloud. Details of these complications and the physics of the new scheme itself are given in [Tompkins et al. \(2007\)](#). In this work, the impact of allowing supersaturation is shown to be that expected; an increase in upper troposphere humidity at the expense of the occurrence and opacity of cirrus ice clouds. [Tompkins et al. \(2007\)](#) also illustrates the improvement of the model with respect to ground-based observations of permanent contrails (a proxy for the existence of a supersaturated air mass) as well as in situ aircraft and remote satellite observations of upper tropospheric humidity and supersaturation.

2.3.2 Convection

A major revision to the convection scheme has been implemented in cycle 32R3. These changes were to introduce a convective entrainment rate that is sensitive to environmental moisture, a deep convection closure where the convective available potential energy is relaxed towards a neutral state using a spatially-varying relaxation time-scale, and a fully implicit numerical formulation. A more detailed description of the convection changes along with their impacts on some aspects of the ECMWF model climate are given in [Bechtold et al. \(2008\)](#).

In cycle 33R1 a constant background entrainment has been added to the relative humidity-dependent entrainment rate in order to reverse the slight degradation in upper-tropospheric tropical winds introduced in cycle 32R3.

2.3.3 Soil hydrology

A revised soil hydrology has been introduced in cycle 33R1 for the Tiled ECMWF Scheme for Surface Exchanges over Land (HTESSEL [Viterbo and Beljaars, 2005](#); [Viterbo et al., 1999](#); [van den Hurk et al., 2000](#); [Balsamo et al., 2008](#)). The revision addressed two main shortcomings of the land surface scheme: the absence of surface runoff and a global uniform soil texture. A new dataset for soil type based on the Food and Agriculture Organization (FAO) was included, and hydrological classes (up to six) were assigned to each grid cell. A revised infiltration scheme with sub-grid surface runoff description was also introduced and evaluated. In point comparisons with field site experiments these modifications show a shift in the soil moisture range to give better agreement with observations. The soil physiographic parameters (wilting point and field capacity) associated to each soil texture produced a larger soil water holding capacity. In drylands the shift of the soil moisture range gave slightly better evaporation. A Boreal forest site was selected for its long time-series of soil moisture observations. The inter-annual variability of root-zone soil moisture showed improvements with a satisfactory match to a 8-year continuous dataset. Quantitative evaluation of the land surface runoff at monthly time-scales shows a net improvement of runoff timing in relevant catchments, when evaluated in a set of regional stand-alone experiments (see [Balsamo et al., 2008](#), for details). Atmospheric coupled hindcasts revealed a small positive impact on the model climate. A reduction of data assimilation increments at the surface was obtained in the IFS for the soil moisture field.

3 Results

3.1 Precipitation

The observed mean precipitation climatology during boreal winter from the Global Precipitation Climatology Project ([Adler et al., 2003](#)) is shown in Figure 1 (upper left panel). The largest values are found in the tropics, particularly over central South America, Africa and the Maritime Continent. In the Northern Hemisphere extratropics the largest mean precipitation is found in North Atlantic and North Pacific storm tracks.

Model cycles 29R2, 30R1 and 31R1 show very similar systematic precipitation errors, both in the tropics and extratropics. In the tropics, precipitation is generally too weak (strong) over the continents (oceans). Positive precipitation biases are particularly problematic in the tropical Atlantic, the southern parts of the Caribbean, the Indian ocean, and just north off the equator in the tropical Pacific. In the North Atlantic/European region precipitation biases are indicative of an underestimation of Euro-Atlantic blocking events and a too weak storm track in higher latitudes (see below, for more details). Interestingly, the above-mentioned precipitation biases have been already present in the ECMWF model for many years (e.g. [Brankovic et al., 2002](#); [Jung and Tompkins, 2003](#)).

Changes in cycle 32R1 (see Table 1), in particular to the radiation scheme, led to a substantial reduction of the “dry bias” over the tropical continents and a reduction of precipitation in the eastern tropical Pacific and the

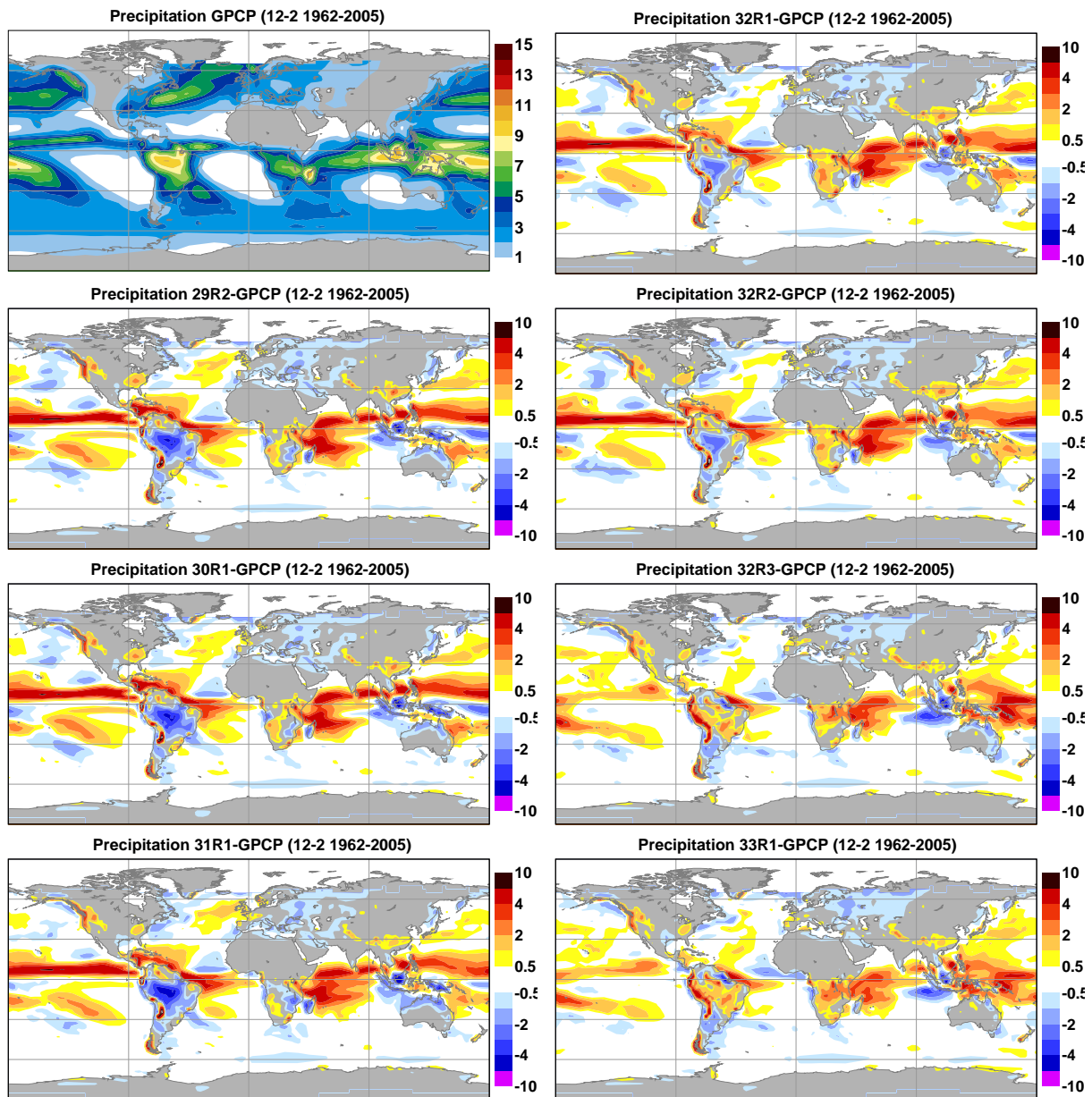


Figure 1: Observed mean precipitation (mm day^{-1}) from GPCP for winters (December–February) of the period 1979–2001 (upper left panel) along with systematic precipitation errors for various cycles of the ECMWF model (from top to bottom and left to right). Model climatologies have been computed using data from 1962–2005.

tropical Atlantic/Caribbean.

The largest change of systematic precipitation errors occurred from cycle 32R2 to 32R3. These changes were mostly beneficial in the sense that they led to reduced systematic precipitation errors, particularly in the tropical Pacific, on the northern flank of the Maritime Continent, in the Caribbean and over central South America. Additional sensitivity experiments have revealed that it was the change to the convection scheme in cycle 32R3, which was responsible for these changes. In summary, substantial improvements in the representation of climatological mean precipitation has been achieved in the ECMWF model during the period 2005–2008. Even for the latest model cycles, however, there are still substantial systematic errors in simulating mean precipitation including too much precipitation in the tropical Indian ocean, the western tropical Pacific.

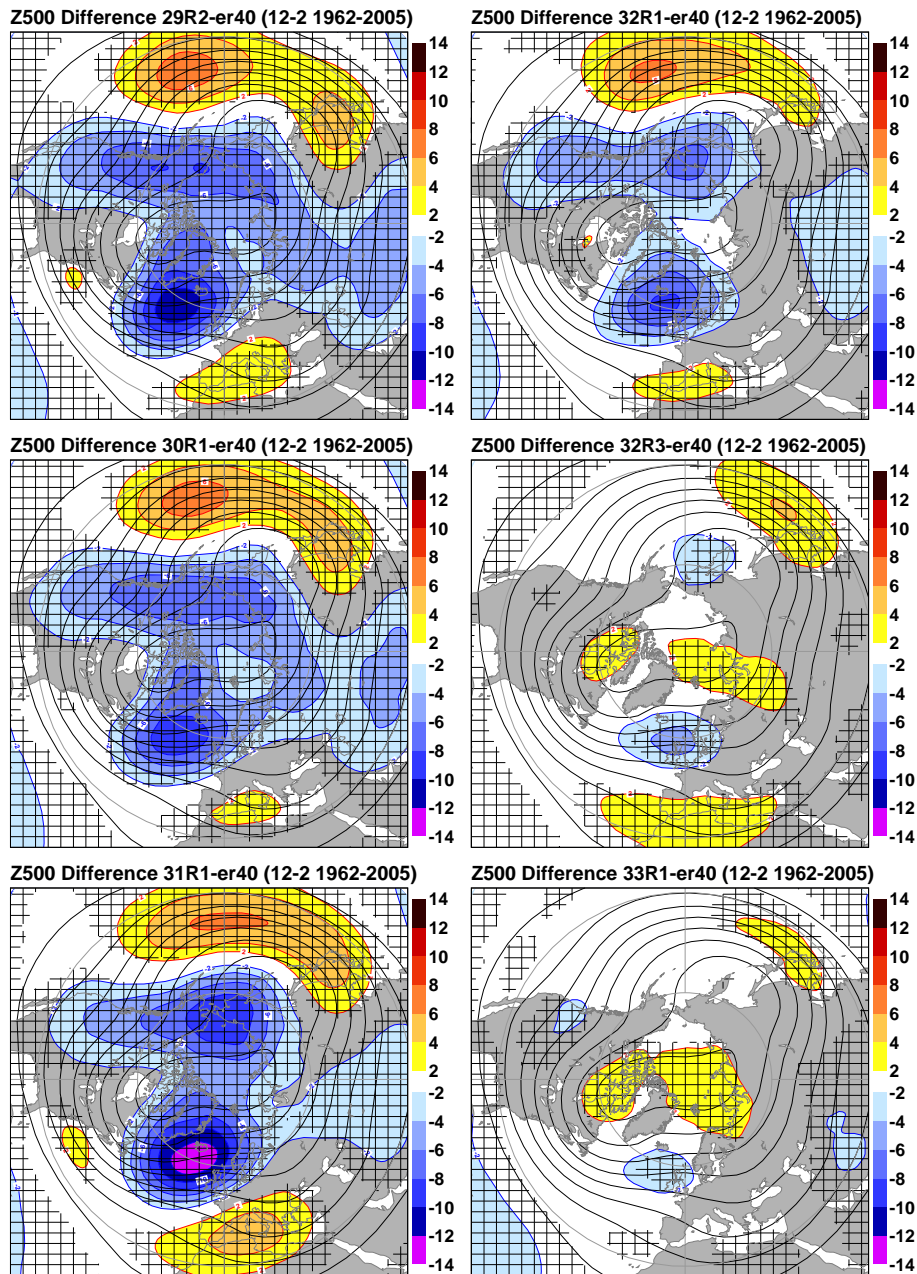


Figure 2: Mean systematic error of 500 hPa geopotential height fields (shading in dam) for winters (December–February) of the period 1962–2005 and various cycles of the ECMWF model (from top to bottom and left to right). Also shown are mean fields (contours) obtained from a combination of ERA-40 (1962–2001) and operational ECMWF analysis data (2002–2005). Mean systematic errors significant at the 95% confidence level are hatched.

3.2 Extratropical circulation

Figure 2 shows how recent model improvements have changed the mean atmospheric circulation, in terms of 500 hPa geopotential height fields (Z500, hereafter) in the Northern Hemisphere extratropics during boreal winter. Very similar errors—reflecting a too strong zonal flow—are found for model cycles 29R2 to 32R2. In fact, even for earlier model cycles a very similar systematic error structure was found for Z500 (Brankovic et al., 2002; Jung, 2005). With the introduction of model cycle 32R3 in November 2007 systematic Z500 error in the North Pacific/North America region reduced substantially. Results for the Southern

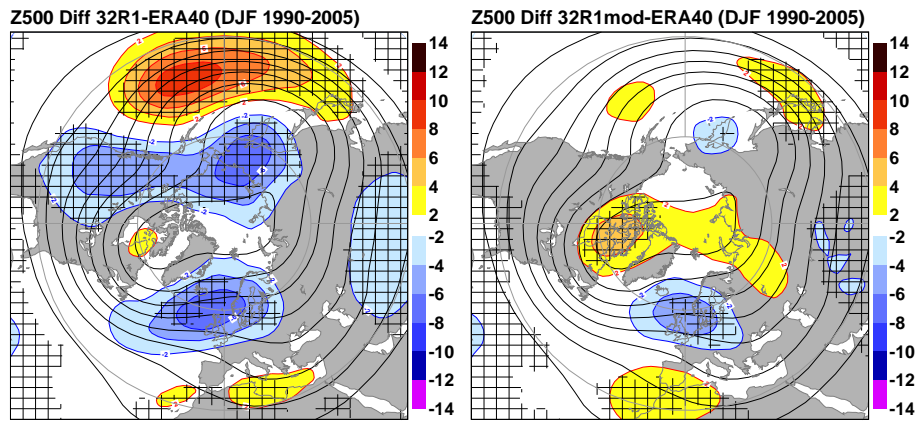


Figure 3: As in Fig. 2, but for model cycle 32R1 with convection formulation taken from (left) 32R1 and (right) 32R3.

Hemisphere (not shown) indicate that recent model changes had a less dramatic influence, which can partly be explained by the fact that older model cycles such as 29R2 and 31R1 has smaller systematic Z500 errors to start with.

Systematic Z500 error in the North Atlantic region also underwent substantial changes throughout the period 2005–2008 (Figure 2). Generally, the circulation was too cyclonic from model cycle 29R2 to 32R2. In cycle 31R1 this error was further enhanced due to an excessively strong stratospheric polar vortex in the 91 level version of the model which was a result of a too weak drag exerted by the SSO gravity wave parametrization in the stratosphere (Orr, 2007).

Additional experimentation for winters of the period 1990–2005 using model cycle 32R1 with the original and the new convection formulation introduced in 32R3 shows that it was the modification of the convection scheme in cycle 32R3 (Table 1), which led to the reduction of systematic Z500 error in the North Pacific and over North America (Figure 3). Similarly, improvements in the North Atlantic region in cycle 32R3 can be traced back primarily to changes to the convection scheme. This interpretation is confirmed by additional sensitivity experiments with cycle 32R3 with and without the new vertical diffusion scheme (not shown). Rossby wave source diagnostics (Sardeshmukh and Hoskins, 1988) (not shown) suggest that the reduction of systematic Z500 error over the Northern Hemisphere is due to a better representation of the diabatic heating in the tropics, particularly at the northern flank of the Maritime Continent, the central tropical Pacific, central South America, the Caribbean and the tropical Atlantic (see also Figure 1).

3.3 Blocking

The capability of models to capture the observed frequency of blocking events is crucial, given the importance of blocking for local weather conditions. This is particularly true for Europe where, during wintertime, blocking events lead to an interruption of the predominantly mild southwesterly winds. It is well-known that many climate models underpredict the observed frequency of occurrence of blocking, particularly in the Euro-Atlantic region (e.g., D'Andrea et al., 1998; Boyle, 2006). The same is certainly true for earlier versions of the ECMWF model (e.g. Jung, 2005).

The observed and simulated frequency of occurrence of Northern Hemisphere blocking using model cycles 29R2 to 33R1 are shown in Figure 4 for winters of the period 1962–2005 (upper panel). Here, blocking frequencies were computed using the method introduced by Tibaldi and Molteni (1990). The observations show two well-known maxima in the North Pacific and Euro-Atlantic region. In the North Pacific region simulated blocking frequencies were substantially underestimated until the introduction of model cycle 32R3 (blue and red curves). The same is true for the Euro-Atlantic region. It is worth pointing that in the Euro-Atlantic region, for the first time, it is possible to obtain realistic blocking frequencies in climate sim-

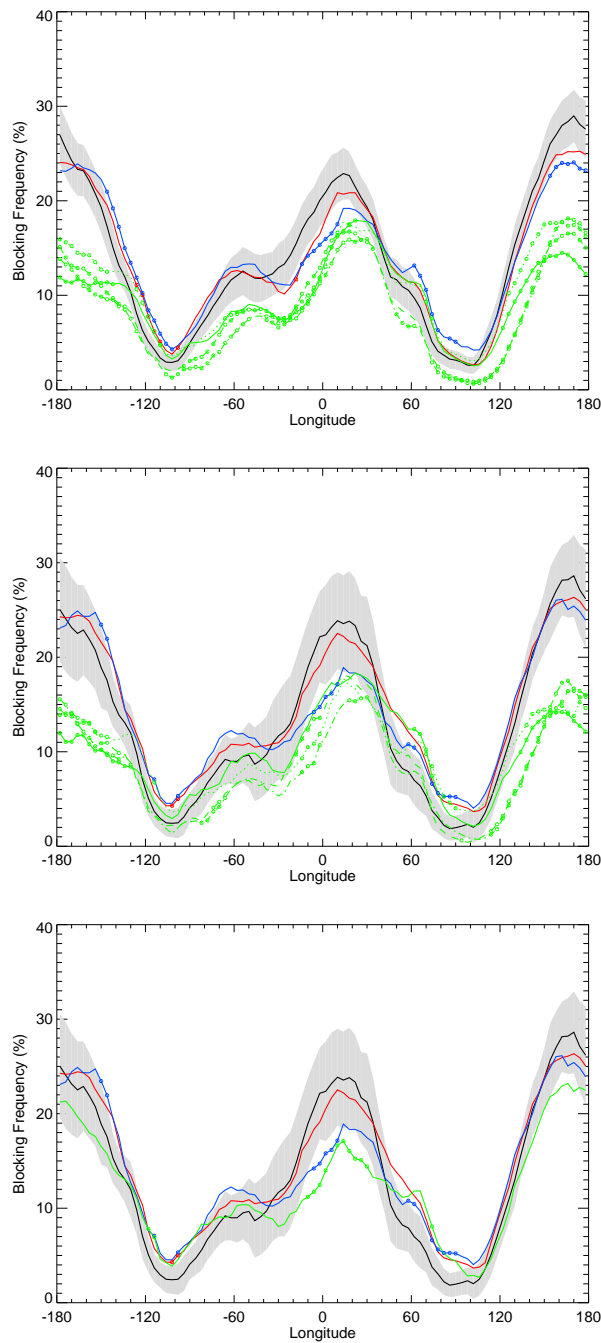


Figure 4: Frequency of occurrence of wintertime Northern Hemisphere blocking events (December–February). Upper panel: ERA-40 (black), cycle 33R1 (red), cycle 32R3 (blue) and cycles 29R2–32R2 (green) for the period 1962–2005. Middle panel: As Upper panel, but for the period 1990–2005. Lower panel: ERA-40 (black), cycle 33R1 (red), cycle 32R3 (blue) and cycle 33R1 with reduced orographic form drag (green). Blocking frequencies have been determined using the methodology suggested by Tibaldi and Molteni (1990). Longitudes for which the modeled blocking frequency differs significantly (at the 95% confidence level) from ERA-40 data are marked by filled circles. Also shown are 95% confidence intervals for ERA-40 data (grey shading).

ulations with cycle 32R3 and 33R1. In the North Pacific region, on the other hand, similar improvements have been previously achieved by the introduction of a more realistic aerosol climatology in October 2003 (Rodwell and Jung, 2008) (the error re-appeared in the following model cycle) and by implementing a stochas-

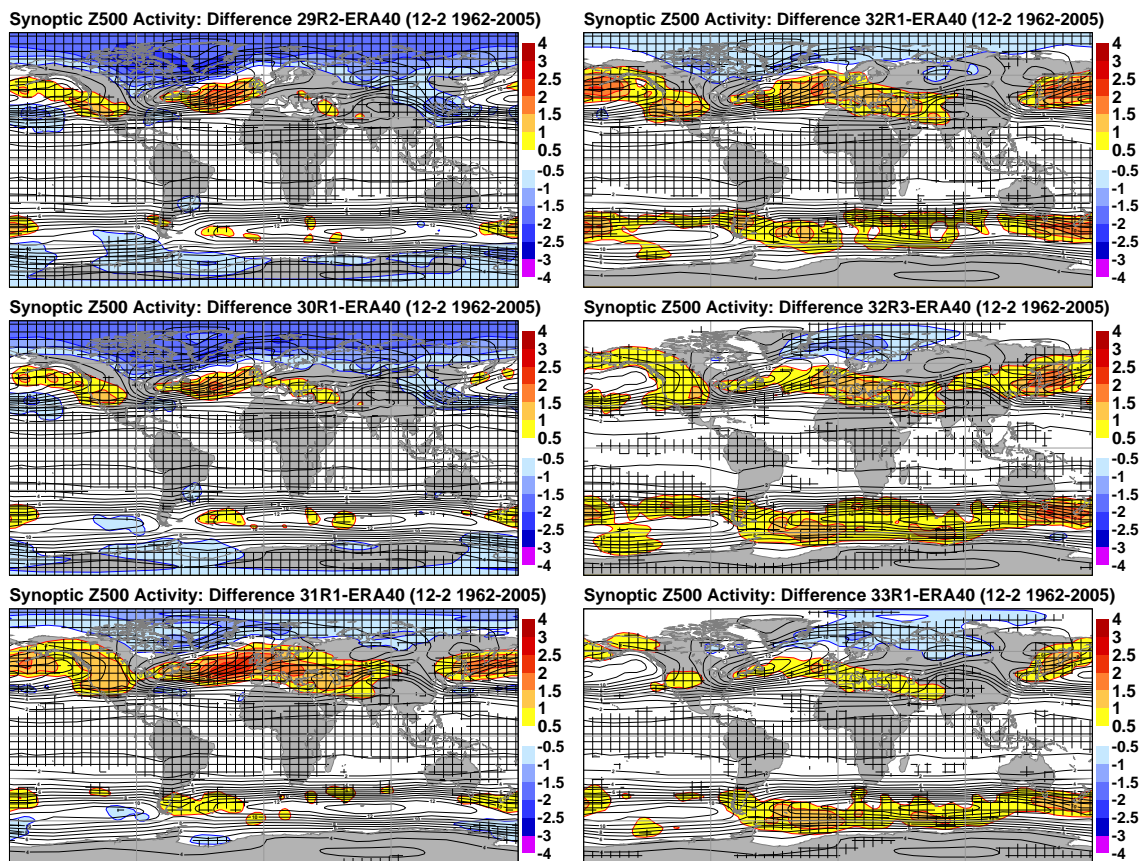


Figure 5: As in Fig. 2, but for synoptic activity of 500 hPa geopotential height fields (shading in m day^{-1}). “Synoptic activity” is defined as the standard deviation of highpass-filtered Z500 fields. Here a tendency filter was used in order to carry out the highpass-filtering (see Jung, 2005, for details).

tic parametrization (Jung et al., 2005a). The fact that differences in the blocking frequencies between model cycle 29R2 to 32R2 are much smaller than the impact that the introduction for cycle 32R3 highlights the significance of these model improvements.

The middle panel of Figure 4 shows the same diagnostics as the upper panel, but for the shorter period 1990–2005 for which sensitivity experiments are available. A direct comparison of the observed blocking frequency between the two periods shows evidence for pronounced decadal-scale changes in the Euro-Atlantic; the anomalously weak westerly flow during the 1960s and early 1970s, associated with the predominantly negative phase of the North Atlantic Oscillation (NAO) (e.g. Hurrell, 1995), clearly led to more blocking episodes over the North Atlantic around 60°W . From 1990–2005, on the other, blocking occurred more frequently than normal over Europe. The general conclusion drawn for the sub-period 1990–2005 are similar to those for the full period 1962–2005, that is, the simulated blocking frequency has been significantly improved with the introduction of cycle 32R3. There are differences, however, associated with blocking over Europe, where 33R1 performs significantly better than 32R3. An additional sensitivity experiment with cycle 33R1, in which a lower turbulent orographic form drag (employed in earlier model cycles) was used, shows that the increased turbulent orographic for drag leads to an increased—and more realistic—frequency of occurrence of Euro-Atlantic blocking events.

3.4 Synoptic activity

Previous studies have revealed that older versions of the ECMWF model underestimate the level of synoptic activity in high latitudes of the Northern Hemisphere in climate integrations (Jung, 2005), particularly at relatively low horizontal resolutions (Jung et al., 2006) such as the one employed in this study (i.e., T_L159). Figure 5 shows systematic errors in synoptic activity of daily Z500 fields for model cycles 29R2 to 33R1 (see caption for details on how synoptic activity is defined). Two major improvements stand out. First, the introduction of cycle 31R1 led to a higher, and more realistic levels of synoptic activity in the high-latitudes of the Northern Hemisphere. One possible explanation for this improvement is the revision to the cloud scheme (in particular the more realistic treatment of ice supersaturation). Without further sensitivity experiments (not available at the moment), however, it is difficult to pinpoint the exact cause for this change. Second, there was a distinct improvement over the Northern Hemisphere with the introduction of cycle 32R3 (Figure 5), particularly in the North Pacific region. Additional experiments reveal that the improvement over the Northern Hemisphere can be explained by changes to the convection scheme (not shown). This is consistent with the results obtained for mean Z500 fields (Figure 3).

In the Southern Hemisphere the level of synoptic Z500 activity seems to have deteriorated (in the sense of the model being overactive) with the introduction of cycle 32R1 (Figure 5). Whether this change reflects a true deterioration or just the fact that analysis data are largely influenced by the first guess (and hence the model used in the ERA-40 reanalysis), particularly in the pre-satellite era, remains to be shown.

3.5 Convectively coupled tropical waves

Previous studies show that current state-of-the-art general circulation models still have significant problems and display a wide range of skill in simulating convectively coupled tropical waves (e.g. Lin et al., 2006). In the following, convectively coupled tropical waves are diagnosed using the technique of Wheeler and Kiladis (1999), that is, wavenumber-frequency spectra are computed for observed and simulated anomalies of outgoing long-wave radiation (OLR); here, the focus is on the symmetric component (about the equator). In the observations more power is located in the eastward propagating Kelvin wave part, including the Madden-Julian oscillation (MJO), than in the westward propagating Rossby wave part (Figure 6, upper left panel). In the ECMWF model the opposite is true for model cycles 29R2 to 32R2. With the introduction of model cycle 32R3, however, the wavenumber-frequency characteristics of the ECMWF model became much more realistic (see also Bechtold et al., 2008).

It is worth trying to understand the changes seen with the introduction of model cycle 32R3 in some more detail. The left panels of Figure 7 show wavenumber-frequency diagrams for the symmetric component of tropical precipitation anomalies in cycle 32R2 for the large-scale (upper panel) and convective (lower panel) part. In cycle 32R2, large-scale (convective) tropical precipitation anomalies are dominated by eastward (westward) propagating Kelvin (Rossby) waves. One might speculate, therefore, that the changes that occurred with the introduction of cycle 32R3 (primarily changes to the convection scheme) are due to an increase in the relative contribution of the large-scale scheme to the total precipitation (see Tompkins and Jung, 2004, for a discussion of this topic). The right panel of Figure 7, which depicts corresponding diagnostics for cycle 32R3, shows that this is not the case. In fact, in cycle 32R3 the convective precipitation scheme has a much larger contribution to total precipitation anomalies than in previous cycles. Moreover, the *structure* of the wavenumber-frequency spectrum for convective precipitation has changed in cycle 32R3; with Kelvin waves playing a much more important role. The reason for these changes, however, is not yet fully understood and is subject of ongoing research.

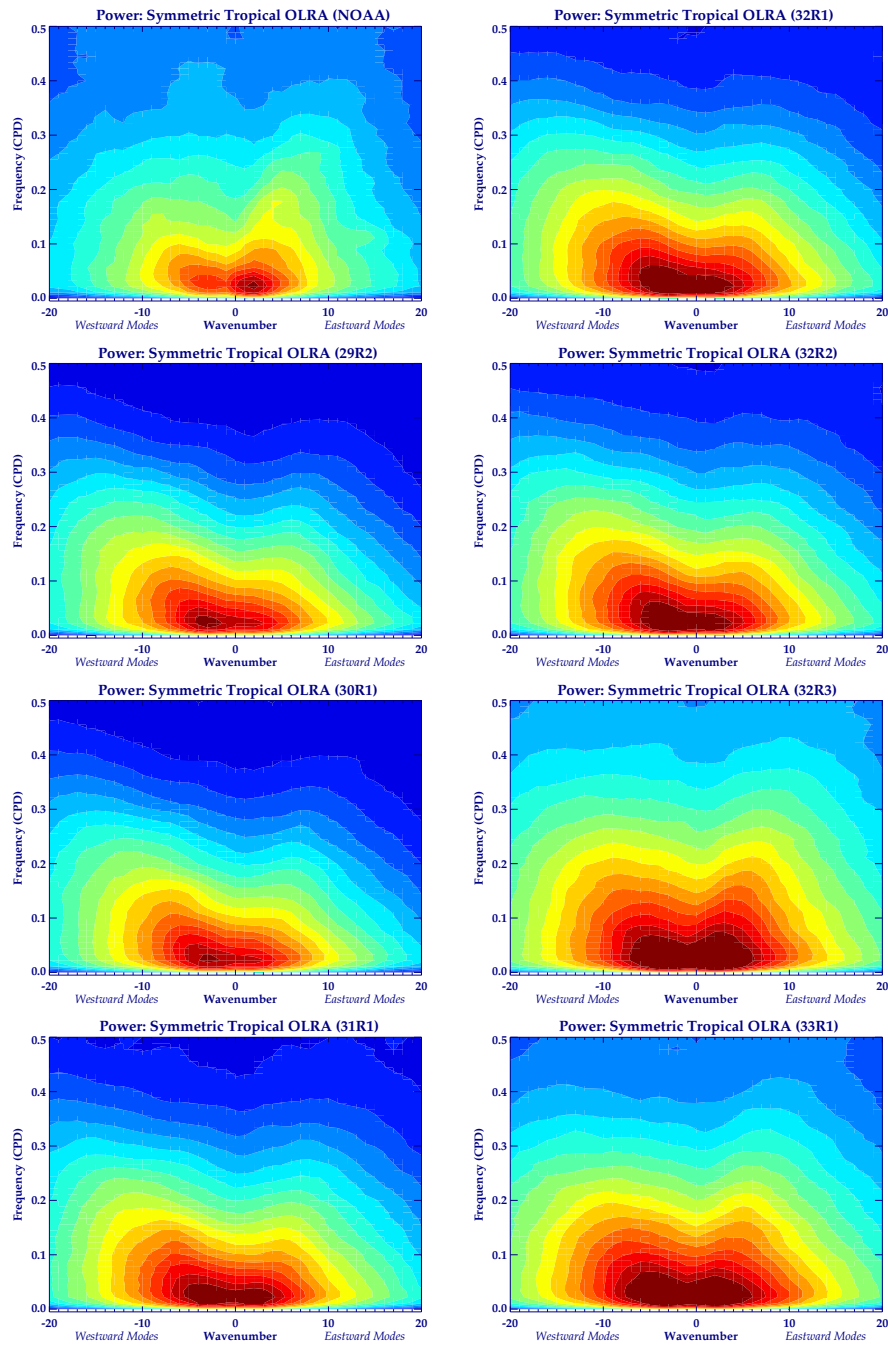


Figure 6: Mean wavenumber-frequency diagrams of the symmetric component of tropical outgoing long-wave radiation anomalies (K^2) during wintertime (December–February) from twice-daily satellite and data (1990–2005) and various cycles of the ECMWF model (1962–2005). The mean annual cycle has been removed prior to the computation of the wavenumber-frequency spectra.

3.6 The North Atlantic Oscillation

It is well-known that the dominant ‘regimes’ of atmospheric variability over the Northern Hemisphere such as the Pacific North American pattern and the North Atlantic Oscillation (NAO) have large impacts on climate in densely populated regions such as North America and Europe (e.g. van Loon and Rogers, 1978). Moreover, there is evidence that the atmospheric response to increasing greenhouse gases may manifest itself primarily through a change in the frequency of occurrences of some of the regimes (e.g. Hurrell, 1996; Palmer, 1999;

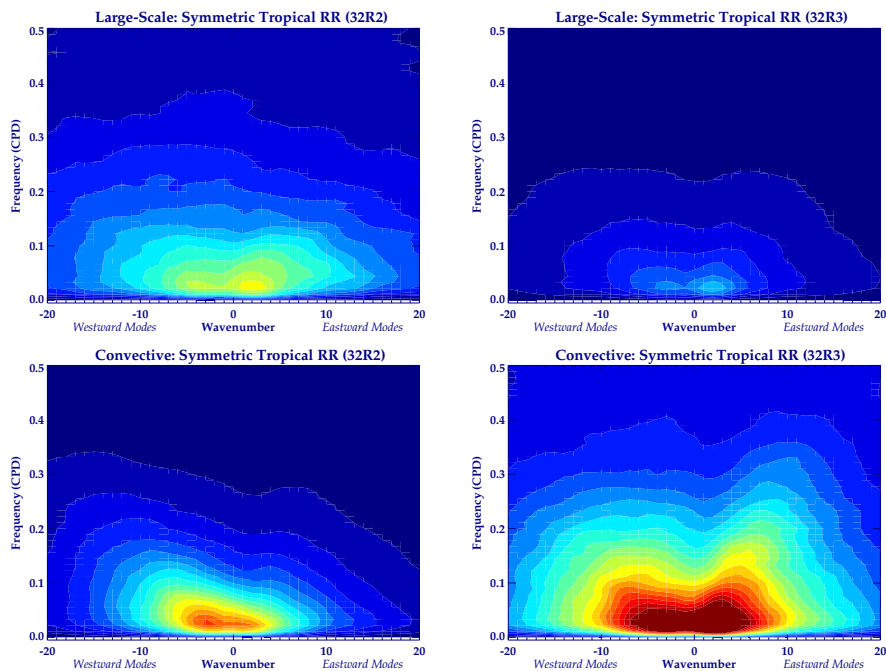


Figure 7: As in Fig. 6, but for large-scale (upper panels) and convective (lower panels) precipitation separately. Results are shown for model cycle 32R2 (left) and 32R3 (right).

Monahan et al., 2000). Predictions of these regimes on time scales from months to decades are nowadays more or less routinely being carried out using coupled models. An assessment of the Arctic Oscillation, which is related to the NAO in the North Atlantic sector, in the 20th century Intergovernmental Panel on Climate Change Fourth Assessment Report (IPCC AR4) models reveals still substantial short-comings of some state-of-the-art models in simulating observed characteristics of the AO/NAO (Miller et al., 2006).

The spatial structure and percentage of explained variance of the observed NAO and the NAO simulated by the different cycles of the ECMWF model is shown in Figure 8. In general, the agreement of the observed and simulated NAO in the North Atlantic/European region is fairly good; this is particularly true for more recent cycles, even in terms of the remote relationship with the North Pacific region. The largest discrepancy between observed and simulated NAO is found for model cycle 29R2. The improvement for 30R1 suggest (see Table 1) that increasing vertical resolution is beneficial when it comes to simulating the NAO. In summary, it can be said that the representation of the NAO on interannual time scales is very well represented by recent cycles of the ECMWF model.

4 Summary and Discussion

Results from a set of climate runs with recent cycles of the ECMWF model show that improvements of the physical parametrization package since June 2005 led to substantial reduction of many long-standing systematic model errors. Notable improvements include the tropical hydrological cycle, and the atmospheric circulation in the Northern Hemisphere extratropics including extratropical cyclones and the frequency of occurrence of Euro-Atlantic blocking events. Although each upgrade since June 2005 led to distinct improvements of the ECMWF model climate, the biggest change occurred in November 2007, when the convection scheme was substantially modified (see also Bechtold et al., 2008).

Jung et al. (2006) argued that the level of synoptic activity simulated by the ECMWF model is strongly dependent on horizontal resolution and that it is necessary to use resolutions higher than T_L159 in order to obtain

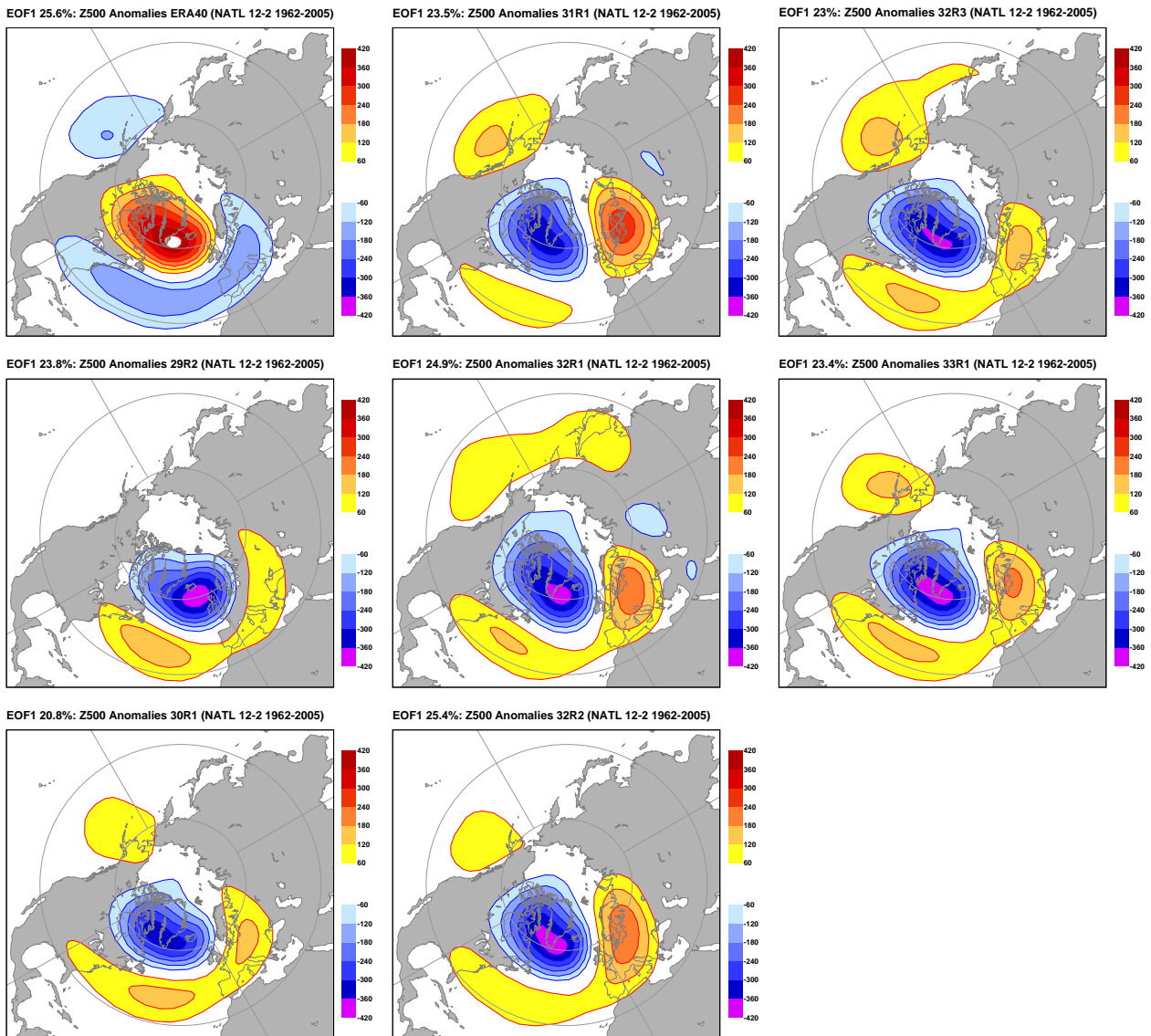


Figure 8: Seasonal mean 500 hPa geopotential height anomalies (in $m^2 s^{-2}$) for winters (December–February) of the period 1962–2005 associated with North Atlantic Oscillation (NAO) index. The NAO index is defined as the principal component (PC) of the leading empirical orthogonal function (EOF) of North Atlantic 500 hPa geopotential height anomalies. Anomalies shown are based on the difference between mean fields for winters with anomalously high (above 1 standard deviation) and low (below -1 standard deviation) PC. Notice, that the sign of the patterns is arbitrary.

a realistic representation of the observed synoptic-scale systems. Their study was based on experimentation with model cycle 29R2. In fact, this study shows, that realistic levels of synoptic activity can be obtained even at a resolution of T_L159 if a better parametrization package is used (see Figure 5).

It is anticipated that the improvements in model climate reported in this study and in [Bechtold et al. \(2008\)](#) will be beneficial for future ECMWF activities such as reanalyses.

While there is no doubt about the fact that the changes to the ECMWF model described in this paper are primarily beneficial there are still some issues which will need to be addressed in the near future. The phase speed and periodicity of the Madden-Julian Oscillation, for example, are still poorly simulated even by the latest model cycle. Moreover, some aspects of the climate have slightly deteriorated such as Indian Summer Monsoon and near-surface zonal winds in the tropical Pacific which tend to lock the coupled atmosphere-ocean

model used at ECMWF to carry out seasonal forecasts in a form of permanent La Nina state (Tim Stockdale, personal communication).

References

- Adler, R. F., J. Susskind, G. Huffman, D. Bolvin, N. E., A. Chang, R. Ferraro, A. Gruber, P.-P. Xie, J. Janowiak, B. Rudolf, S. Schneider, U. Curtis, and P. Arkin, 2003: The version-2 Global Precipitation Climatology Project (GPCP) monthly precipitation analysis (1979–present). *J. Hydromet.*, **4**, 1147–1167.
- Balsamo, G., P. Viterbo, A. Beljaars, B. van der Hurk, M. Hirschi, A. K. Betts, and L. Scipal, 2008: A revised hydrology for the ECMWF model: Verification from field site to terrestrial water storage and impact in the integrated forecast system. *J. Hydrometeor.*, p. submitted.
- Barker, H. W., R. Pincus, and J.-J. Morcrette, 2002: The Monte-Carlo Independent Column Approximation: Application within large-scale models. In: *Extended Abstracts, GCSS/ARM Workshop on the Representation of Cloud Systems in Large-Scale Models*, p. 10pp. Kananaskis, AB, Canada, GEWEX. Available on-line at <http://www.met.utah.edu/skrueger/gcss-2002/Extended-Abstracts.pdf>.
- Bechtold, P., M. Köhler, T. Jung, F. Doblas-Reyes, M. Leutbecher, M. Rodwell, F. Vitart, and G. Balsamo, 2008: Advances in simulating atmospheric variability with the ECMWF model: From synoptic to decadal time-scales. *Quart. J. Roy. Meteor. Soc.*, **134**, 1337–1351.
- Beljaars, A. C. M., P. Bechtold, M. Köhler, J.-J. Morcrette, A. M. Tompkins, P. Viterbo, and N. Wedi, 2004a: The numerics of physical parameterization. In: *Proceedings of ECMWF Seminar on Recent Developments in Numerical Methods for Atmospheric and Ocean Modelling*, pp. 113–134. ECMWF, Shinfield Park, Reading, Berkshire RG2 9AX, UK.
- Beljaars, A. C. M., A. R. Brown, and N. Wood, 2004b: A new parametrization of turbulent orographic form drag. *Quart. J. Roy. Meteor. Soc.*, **130**, 1327–1347.
- Boyle, J. S., 2006: Upper level atmospheric stationary waves in the twentieth century climate of the Intergovernmental Panel on Climate Change simulations. *J. Geophys. Res.*, **111**, doi:10.1029/2005JD006612.
- Brankovic, C., C. Jakob, M. Miller, A. Untch, and N. Wedi, 2002: Climate diagnostics of the ECMWF AMIP-2 simulations. Technical Report 360, Shinfield Park, Reading, Berkshire RG2 9AX, UK.
- D’Andrea, F., S. Tibaldi, M. Blackburn, G. Boer, M. Deque, M. R. Dix, B. Dugas, L. Ferranti, T. Iwasaki, A. Kitoh, D. Pope, V. Randall, E. Roeckner, D. Straus, W. Stern, H. Van den Dool, and D. Williamson, 1998: Northern Hemisphere atmospheric blocking as simulated by 15 atmospheric general circulation models in the period 1979–1988. *Clim. Dyn.*, **14**, 385–407.
- Demott, P. J., D. J. Cziczo, A. J. Prenni, D. M. Murphy, S. M. Kreidenweis, and D. S. Thomson, 2003: Measurements of the concentrations and composition of nuclei for cirrus formation. *Proc. Nat. Acad. Sci.*, **100**, 14655–14660.
- Gierens, K., 2003: On the transition between heterogeneous and homogeneous freezing. *Atmos. Chem. Phys.*, **3**, 437–446.
- Hurrell, J. W., 1995: Decadal trends in the North Atlantic Oscillation: Regional temperatures and precipitation. *Science*, **269**, 676–679.
- Hurrell, J. W., 1996: Influence of variations in extratropical wintertime teleconnections on Northern Hemisphere temperature. *Geophys. Res. Lett.*, **23**, 665–668.

- Iacono, M. J., J. S. Delamere, E. J. Mlawer, M. W. Shephard, S. A. Clough, and W. D. Collins, 2008: Radiative forcing by long-lived greenhouse gases: Calculations with the AER radiative transfer models. *J. Geophys. Res.*, **113**, D13103, doi:10.1029/2008JD009944.
- Jung, T., 2005: Systematic errors of the atmospheric circulation in the ECMWF forecasting system. *Quart. J. Roy. Meteor. Soc.*, **131**, 1045–1073.
- Jung, T., S. K. Gulev, I. Rudeva, and V. Soloviov, 2006: Sensitivity of extratropical cyclone characteristics to horizontal resolution in the ECMWF model. *Quart. J. Roy. Meteor. Soc.*, **132**, 1839–1857.
- Jung, T., T. N. Palmer, and G. J. Shutts, 2005a: Influence of a stochastic parameterization on the frequency of occurrence of North Pacific weather regimes in the ECMWF model. *Geophys. Res. Lett.*, **32**, L23811. Doi:10.1029/2005GL024248.
- Jung, T. and A. M. Tompkins, 2003: Systematic errors in the ECMWF forecasting system. Technical Report 422, ECMWF, Shinfield Park, Reading, Berkshire RG2 9AX, UK. Available at <http://www.ecmwf.int/publications/>.
- Jung, T., A. M. Tompkins, and M. J. Rodwell, 2005b: Some aspects of systematic error in the ECMWF model. *Atmos. Sci. Lett.*, **6**, 133–139.
- Lin, J., N. Kiladis, B. Mapes, K. Weickmann, K. Sperber, W. Lin, M. Wheeler, S. Schubert, A. Del Genio, L. Donner, S. Emori, J.-F. Guérémy, F. Hourdin, P. Rasch, E. Roeckner, and J. Scinocca, 2006: Tropical intraseasonal variability in 14 IPCC AR4 climate models. Part I: Convective signals. *J. Climate*, **19**, 2665–2690.
- Lin, Y. L., R. D. Farley, and H. D. Orville, 1983: Bulk parameterization of the snow field in a cloud model. *J. Climate Appl. Meteor.*, **22**, 1065–1092.
- Lohmann, U. and B. Kärcher, 2002: First interactive simulations of cirrus cloud formed by homogeneous freezing in the ECHAM general circulation model. *J. Geophys. Res.*, **107**, 10.1029/2001JD000767.
- Louis, J. F., M. Tiedtke, and J. F. Geleyn, 1982: A short history of the pbl parameterization at ecmwf. In: *Workshop on Boundary-Layer Parametrizations*, pp. 59–79. ECMWF, Shinfield Park, Reading RG2 9AX, UK.
- Miller, R. L., G. A. Schmidt, and D. T. Shindell, 2006: Forced annular variations in the 20th century Intergovernmental Panel on Climate Change Fourth Assessment Report models. *J. Geophys. Res.*, **111**, D18101, doi:10.1029/2005JD006323.
- Mlawer, E. J., S. J. Taubman, P. D. Brown, M. J. Iacono, and S. A. Clough, 1997: Radiative transfer for inhomogeneous atmospheres: RRTM, a validated correlated-k model for the longwave. *J. Geophys. Res.*, **102**, 16663–16682.
- Monahan, A. H., J. C. Fyfe, and G. M. Flato, 2000: A regime view of Northern Hemisphere atmospheric variability and change under global warming. *Geophys. Res. Lett.*, **27**, 1139–1142.
- Morcrette, J.-J., H. W. Barker, J. N. S. Cole, M. J. Cole, M. J. Iacono, and R. Pincus, 2008a: Impact of a new radiation package, McRad, in the ECMWF integrated forecasting system. *Mon. Wea. Rev.*. In press.
- Morcrette, J.-J., G. Mozdzynski, and M. Leutbecher, 2008b: A reduced radiation grid for the ecmwf integrated forecasting system. Technical Report 538, ECMWF, Shinfield Park, Reading, Berkshire RG2 9AX, UK. Available at <http://www.ecmwf.int/publications/>.
- Orr, A., 2007: Evaluation of revised parameterizations of sub-grid orographic drag. Technical Report 537, ECMWF, Shinfield Park, Reading, Berkshire RG2 9AX, UK. Available at <http://www.ecmwf.int/publications/>.

- Palmer, T. N., 1999: A nonlinear dynamical perspective on climate prediction. *J. Climate*, **12**, 575–591.
- Pincus, R., H. W. Barker, and J.-J. Morcrette, 2003: A fast, flexible, approximate technique for computing radiative transfer in inhomogeneous clouds. *J. Geophys. Res.*, **108D**, 4376, doi:10.1029/2002JD003322.
- Reichler, T. and J. Kim, 2008: How well do coupled models simulate today's climate? *Bull. Amer. Meteor. Soc.*, **89**, 303–311.
- Rodwell, M. J. and T. Jung, 2008: Understanding the local and global impacts of model physics changes: An aerosol example. *Quart. J. Roy. Meteor. Soc.*, **134**, 1479–1497.
- Sardeshmukh, P. D. and B. J. Hoskins, 1988: The generation of global rotational flow by steady idealized tropical divergence. *J. Atmos. Sci.*, **45**, 1228–1251.
- Sundqvist, H., E. Berge, and J. E. Kristjansson, 1989: Condensation and cloud parameterization studies with a mesoscale numerical weather prediction model. *Mon. Wea. Rev.*, **117**, 1641–1657.
- Tibaldi, S. and F. Molteni, 1990: On the operational predictability of blocking. *Tellus*, **42A**, 343–365.
- Tompkins, A. M., 2008: Cloud Parametrization. In: *Workshop on Parametrization of sub-grid physical processes*, p. pp 39. ECMWF, Shinfield Park, Reading, UK, available from <http://www.ecmwf.int/publications>.
- Tompkins, A. M., K. Gierens, and G. Rädcl, 2007: Ice supersaturation in the ECMWF integrated forecast system. *Quart. J. Roy. Meteor. Soc.*, **133**, 53–63.
- Tompkins, A. M. and T. Jung, 2004: Influence of process interactions on MJO-like convective structures in the IFS model. In: *ECMWF/CLIVAR Workshop on Simulation and Prediction of Intra-Seasonal Variability with Emphasis on the MJO*, pp. 103–114. ECMWF, Shinfield Park, Reading RG2 9AX, UK.
- Untch, A., M. Miller, M. Hortal, R. Buizza, and P. Janssen, 2006: Towards a global meso-scale model: The high-resolution system T799L91 and T399L62 EPS. ECMWF Newsletter 108, ECMWF, Shinfield Park, Reading, Berkshire RG2 9AX, UK.
- van den Hurk, B. J. J. M., P. Viterbo, A. C. M. Beljaars, and A. K. Betts, 2000: Offline validation of the ERA-40 surface scheme. Technical Report 295, ECMWF, Shinfield Park, Reading, Berkshire RG2 9AX, UK. Available at <http://www.ecmwf.int/publications/>.
- van Loon, H. and J. C. Rogers, 1978: The seesaw in winter temperatures between Greenland and Northern Europe. Part I: General description. *Mon. Wea. Rev.*, **106**, 296–310.
- Viterbo, P. and A. C. M. Beljaars, 2005: An improved land surface parametrization scheme in the ECMWF model and its validation. *J. Climate*, **8**, 2716–2748.
- Viterbo, P., A. C. M. Beljaars, J.-F. Mahfouf, and J. Teixeira, 1999: The representation of soil moisture freezing and its impact on the stable boundary layer. *Quart. J. Roy. Meteor. Soc.*, **125**, 2401–2426.
- Wheeler, M. and G. Kiladis, 1999: Convectively coupled equatorial waves: Analysis of clouds and temperature in the wavenumber–frequency domain. *J. Atmos. Sci.*, **56**, 374–399.